

Article

Magnetized Particle Motion in γ -Spacetime in a Magnetic Field

Ahmadjon Abdujabbarov ^{1,2,3,4,5}, Javlon Rayimbaev ^{2,3,4} , Farruh Atamurotov ^{2,6}
and Bobomurat Ahmedov ^{2,3,5,*} 

¹ Shanghai Astronomical Observatory, 80 Nandan Road, Shanghai 200030, China; ahmadjon@astrin.uz

² Ulugh Beg Astronomical Institute, Astronomicheskaya 33, Tashkent 100052, Uzbekistan; javlon@astrin.uz (J.R.); atamurotov@yahoo.com (F.A.)

³ Physics Faculty, National University of Uzbekistan, Tashkent 100174, Uzbekistan

⁴ Institute of Nuclear Physics, Ulughbek, Tashkent 100214, Uzbekistan

⁵ Tashkent Institute of Irrigation and Agricultural Mechanization Engineers, Kori Niyoziy, 39, Tashkent 100000, Uzbekistan

⁶ School of Computer and Information Engineering, Inha University in Tashkent, Tashkent 100170, Uzbekistan

* Correspondence: ahmedov@astrin.uz

Received: 15 September 2020; Accepted: 13 October 2020; Published: 29 October 2020



Abstract: In the present work we explored the dynamics of magnetized particles around the compact object in γ -spacetime in the presence of an external asymptotically-uniform magnetic field. The analysis of the circular orbits of magnetized particles around the compact object in the spacetime of a γ -object immersed in the external magnetic field has shown that the area of stable circular orbits of magnetized particles increases with the increase of γ -parameter. We have also investigated the acceleration of the magnetized particles near the γ -object and shown that the center-of-mass energy of colliding magnetized particles increases with the increase of γ -parameter. Finally, we have applied the obtained results to the astrophysical scenario and shown that the values of γ -parameter in the range of $\gamma \in (0.5, 1)$ can mimic the spin of Kerr black hole up to $a \simeq 0.85$, while the magnetic interaction can mimic the γ -parameter at $\gamma \in (0.8, 1)$ and spin of a Kerr black hole up to $a \simeq 0.3$.

Keywords: γ -object; magnetized particle motion; magnetic field; constraints on black hole parameters

1. Introduction

The Kerr black hole (BH) geometry changes the structure of the asymptotically-uniform magnetic field in its close vicinity [1]. The pioneering work of Wald [1] has initiated the study of properties of the electromagnetic field around axial-symmetric BHs and magnetized neutron stars (see, e.g., [2–19]).

There is current interest in the study of the energetic processes around the BH in modern relativistic astrophysics. Namely, the Penrose process [20], Blandford–Znajek mechanism [21], magnetic Penrose process [22–25] and particle acceleration mechanism (BSW) [26] have been developed. These mechanisms can be used to explain the high energetic particle extraction from active galactic nuclei (AGNs) where supermassive black holes could be located. Motivated by this, the energetic processes around BHs in different scenarios in extended theories of gravity have been recently studied in [4,5,9,27–35].

Rapidly rotating Kerr BH can also play the role of particle accelerator [26]. The energy of colliding particles near the horizon of an extremely rotating black hole can even diverge. On the other hand, an external magnetic field surrounding the BH may have repulsive behavior similar to the rotation parameter of BH and generate an electric field accelerating the charged particles [6,28]. The particles acceleration near the BH has been extensively studied in references [30,36–64]. The energetic processes

around BHs in the presence of an external magnetic field have been explored in [22–25,65–68]. Other astrophysical properties of gravitational compact objects in the presence of a magnetic field have been studied in references [69–71].

The formalism of studying the motion of particles with a nonzero magnetic dipole moment around weakly magnetized Schwarzschild BH was first proposed in Reference [72]. This study has been extended to the rotating Kerr BH case in [73]. The magnetized particle dynamics around BH in alternate theories of gravity have been studied by several authors [50,74–81].

Here we consider the magnetized particle motion and acceleration in the spacetime of the non-rotating compact object described by the so-called γ -metric (also known as the Zipoy–Voorhees spacetime metric) [82,83]. Recently this spacetime metric has been extended to the case of the presence of the scalar field in Reference [84]. The particle motion characteristics in the accretion disc of a BH can be used to develop new tests of gravity theories in a strong field regime [85]. The alternative BH solutions, which can mimic the standard general relativistic solutions have been investigated in [86–91]. Here we study how the γ -parameter of the spacetime together with magnetic interaction can mimic the rotation parameter of Kerr BH. In γ spacetime the $r = 2M$ corresponds to the infinitely red-shifted surface rather than event horizon in the Schwarzschild BH spacetime.

The closest S2 star orbiting around Sgr A* is at the distance of about 1000 Schwarzschild radii and its motion definitely cannot be used to test the spin of the BH because the effects of dragging of inertial frames decay as $1/r^3$ with the distance from the central object. However, magnetized neutron stars could be treated as magnetized test particles in supermassive BH (SMBH) close environment where the effect of dragging of inertial frames is measurable. Unfortunately, there is no radio pulsar observed near the Sgr A* due to scattering of radio signals in the plasma medium surrounding the SMBH Sgr A*. Moreover, stable orbits could not be allowed for the magnetized objects due to the destructive behavior of the magnetic interaction between the magnetic dipole moment of the radio pulsar and ambient magnetic field. On the other hand, the stability of the magnetized particle orbits depends on the parameters of the considered theory of gravity. However, the dynamics of the test of magnetized particles around compact objects leading to the degeneracy between the parameters of alternate theories of gravity and spin parameter of Kerr BH through the innermost stable circular orbit (ISCO) measurements are studied in [79–81,92,93].

Here we study the electromagnetic field structure and dynamics of magnetized particles around a weakly magnetized γ object. The paper is organized as follows. Section 2 is devoted to studying the test electromagnetic field around the compact object in γ -spacetime. In this section we also study and analyze the magnetized particles motion. We discuss possible astrophysical applications of the obtained results in Section 3. We apply the obtained results to study the acceleration mechanisms around a compact object in γ spacetime in the presence of an external magnetic field in Section 4. The concluding remarks are presented in Section 5.

In this paper we use a spacelike signature $(-, +, +, +)$ for the spacetime and system of geometric units where $G = c = 1$ (however, for an astrophysical application, we have written the speed of light explicitly in our main resulting expressions). Latin indices run from 1 to 3 and Greek ones from 0 to 3.

2. Magnetized Particles Motion in Spacetime of Weakly Magnetized γ -Object

In the present work we assume that the energy of the magnetic field is much smaller than the energy of the gravitational field, so that the effect of the magnetic field is negligibly small to change the background spacetime geometry. We will start with the study of gravitational field effects on the electromagnetic field structure created by an asymptotically-uniform magnetic field. The electromagnetic field structure in γ -spacetime has recently been studied in our preceding paper [34]. In spherical coordinates (t, r, θ, ϕ) the deformed γ -spacetime metric can be expressed as [82,83]

$$ds^2 = g_{tt}dt^2 + g_{rr}dr^2 + g_{\theta\theta}d\theta^2 + g_{\phi\phi}d\phi^2, \quad (1)$$

where the components of the metric tensor are defined as

$$\begin{aligned} g_{tt} &= -f^\gamma, \\ g_{rr} &= f^{\gamma^2-\gamma-1} \left(f + \frac{M^2}{r^2} \sin^2 \theta \right)^{1-\gamma^2}, \\ g_{\theta\theta} &= r^2 f^{\gamma(\gamma-1)} \left(f + \frac{M^2}{r^2} \sin^2 \theta \right)^{1-\gamma^2}, \\ g_{\phi\phi} &= r^2 \sin^2 \theta f^{1-\gamma}, \end{aligned} \quad (2)$$

with the metric function $f = 1 - 2M/r$ and mass density parameter γ , which corresponds to the axial symmetric deformation. The case $\gamma = 1$ corresponds to the well known Schwarzschild solution.

We would like to underline that the γ -spacetime is an exact analytical axial-symmetric solution of Einstein's gravitational field equations for static objects. The spacetime is not spherically symmetric for all values of the γ -parameter and it is spherically symmetric only when $\gamma = 1$ when the solution turns to the Schwarzschild one. The external magnetic field created by the electric current of charged particles in the accretion disk can be approximated as a uniform one between the central black hole and accretion disk near the location of the ISCO radius. In the literature, several authors have studied the nonlinear Einstein–Maxwell system where the electromagnetic field energy density is comparable with the matter energy density, which has more academic interest. In the real astrophysical situation, the electromagnetic field is a test one, and we have explored magnetized particle dynamics in the given gravitational background where the electromagnetic field does not change the spacetime.

2.1. Compact Object Immersed in Uniform Magnetic Field

In Reference [94], we have found the exact analytical solution for the four-potential of the electromagnetic field around a compact object in γ -spacetime immersed in an external asymptotically uniform magnetic field. Using the existence of timelike and spacelike Killing vectors and Lorentz gauge ($\nabla_\alpha A^\alpha = 0$) one may use the Wald approach [1] in order to find the potential A_α of the electromagnetic field in the following form

$$A_t = A_r = A_\theta = 0, \quad A_\phi = \frac{1}{2} B f^{1-\gamma} r^2 \sin^2 \theta, \quad (3)$$

where B is the external magnetic field. The nonzero components of the electromagnetic field tensor expressed through the magnetic field measured by a proper observer have the following form

$$F_{r\phi} = B \sin^2 \theta f^{-\gamma} [r - (\gamma + 1)M], \quad (4)$$

$$F_{\theta\phi} = B r^2 f^{1-\gamma} \sin \theta \cos \theta. \quad (5)$$

Finally, one can easily find the non-vanishing orthonormal radial and azimuthal components of the magnetic field in the following form

$$B^{\hat{r}} = B \cos \theta \left(f + \frac{M^2}{r^2} \sin^2 \theta \right)^{\frac{\gamma^2-1}{2}}, \quad (6)$$

$$B^{\hat{\theta}} = B \sin \theta f^{\frac{1-\gamma^2}{2}} \left(f + \frac{M^2}{r^2} \sin^2 \theta \right)^{\frac{\gamma^2-1}{2}}. \quad (7)$$

Figure 1 demonstrates the influence of the γ -parameter of spacetime on the external asymptotically uniform magnetic field structure around a compact gravitational γ -object. One may see that when $\gamma < 1$ the structure of the magnetic field takes the Meissner-like structure and is expelled from the

gravitational object. In the case when $\gamma > 1$ the magnetic field around γ -object changes its structure from an asymptotically uniform one to the parabolic one.

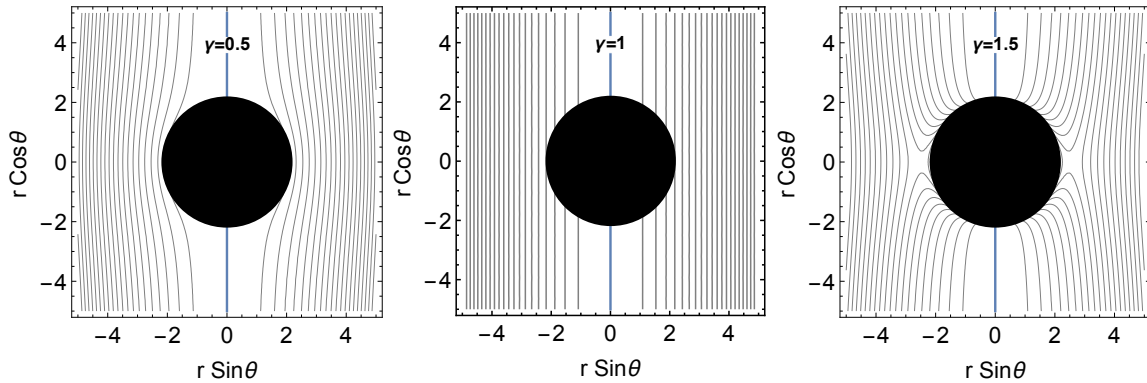


Figure 1. Profiles of magnetic field lines around compact γ -object for the different values of the γ -parameter. The magnetic field is expelled from the surface of infinite red-shift when $\gamma < 1$ and became a parabolic one when $\gamma > 1$. The left panel is for $\gamma = 0.5$, the middle one is for $\gamma = 1$ and the right panel is for $\gamma = 1.5$.

2.2. Magnetized Particles Motion

Now we consider the motion of a particles with a nonzero magnetic dipole moment around a compact object in γ -spacetime embedded in an external asymptotically-uniform magnetic field. We use the Hamilton–Jacobi equation in order to obtain magnetized particles equations of motion, which can be expressed as [72]

$$g^{\mu\nu} \frac{\partial S}{\partial x^\mu} \frac{\partial S}{\partial x^\nu} = - \left(m - \frac{1}{2} D^{\mu\nu} F_{\mu\nu} \right)^2, \quad (8)$$

where $D^{\mu\nu} F_{\mu\nu}$ characterizes the interaction of the external magnetic field with the magnetized particle. Polarization tensor $D^{\alpha\beta}$ is given in the following form [72]

$$D^{\alpha\beta} = \eta^{\alpha\beta\sigma\nu} u_\sigma \mu_\nu, \quad D^{\alpha\beta} u_\beta = 0, \quad (9)$$

where μ^ν is the four-vector of the magnetic dipole moment and u^ν is the four-velocity of the particle. The electromagnetic field tensor $F_{\alpha\beta}$ can be decomposed through electric E_α and magnetic B^α fields in the following form

$$F_{\alpha\beta} = 2u_{[\alpha} E_{\beta]} - \eta_{\alpha\beta\sigma\gamma} u^\sigma B^\gamma. \quad (10)$$

Now the interaction term $D^{\alpha\beta} F_{\alpha\beta}$ can be calculated as [73]

$$D^{\alpha\beta} F_{\alpha\beta} = 2\mu^\alpha B_\alpha = 2\mu B \mathcal{L}[\lambda_{\hat{\alpha}}], \quad (11)$$

where μ is the magnetic moment of the particle and $\mathcal{L}[\lambda_{\hat{\alpha}}]$ is a function of the spacetime coordinates and spacetime parameters, the tetrad $\lambda_{\hat{\alpha}}$ is attached to the co-moving fiducial observer.

Now we will study the motion of magnetized particles around γ -object immersed in an external uniform magnetic field. We consider weak electromagnetic field approximation where $(D^{\mu\nu} F_{\mu\nu})^2 \rightarrow 0$. At the equatorial plane ($\theta = \pi/2$) the equations of motion for magnetized particles can be expressed as

$$\dot{t} = \frac{\mathcal{E}}{f^\gamma}, \quad (12)$$

$$\dot{r}^2 = \mathcal{E}^2 - f^{2\gamma-1} \frac{l^2}{r^2} - (1 - \beta \mathcal{L}[\lambda_{\hat{a}}]) f^\gamma, \quad (13)$$

$$\dot{\phi} = \frac{l}{r^2} f^{\gamma-1}, \quad (14)$$

where “dot” represents derivative with respect to an affine parameter along a particle’s trajectory, specific energy \mathcal{E} and specific angular momentum l are normalized to the mass of the magnetized particle. Using the definition of the effective potential of radial motion

$$\dot{r}^2 = \mathcal{E}^2 - 1 - 2V_{\text{eff}}(r, \gamma, l, \beta), \quad (15)$$

one may easily find the expression for the effective potential of radial motion of the magnetized particle as

$$V_{\text{eff}}(r, \gamma, l, \beta) = \frac{1}{2} \left[f^\gamma \left(1 + f^{\gamma-1} \frac{l^2}{r^2} - \beta \mathcal{L}[\lambda_{\hat{a}}] \right) - 1 \right], \quad (16)$$

where $\beta = 2\mu B/m$ is the magnetic coupling parameter and its value for the case when the magnetized neutron star treated as a test magnetized particle with magnetic dipole moment $\mu_{\text{NS}} = (1/2)B_{\text{NS}}R_{\text{NS}}^3$ orbiting around an SMBH can be calculated as:

$$\beta = \frac{B_{\text{NS}}R_{\text{NS}}^3 B_{\text{ext}}}{m_{\text{NS}}}. \quad (17)$$

Now we will estimate the value of the β parameter in a realistic situation when a neutron star with mass $m_{\text{NS}} = 1.4 M_\odot$, radius $R_{\text{NS}} = 10^6$ cm and the surface magnetic field $B_{\text{NS}} = 10^{12}$ G is orbiting around an SMBH in the presence of an external magnetic field as

$$\beta \simeq \frac{2}{10^3} \left(\frac{B_{\text{NS}}}{10^{12} \text{ G}} \right) \left(\frac{R_{\text{NS}}}{10^6 \text{ cm}} \right)^3 \left(\frac{B_{\text{ext}}}{10 \text{ G}} \right) \left(\frac{m_{\text{NS}}}{1.4 M_\odot} \right)^{-1}. \quad (18)$$

For example, the value of the magnetic coupling parameter β for the magnetar SGR (PSR) J1745–2900 ($\mu \simeq 1.6 \times 10^{32} \text{ G} \cdot \text{cm}^3$ and $m_{\text{NS}} \simeq 1.5 M_\odot$) orbiting the SMBH Sgr A* [95] is

$$\beta_{\text{PSRJ1745-2900}} \simeq 0.716 \left(\frac{B_{\text{ext}}}{10 \text{ G}} \right). \quad (19)$$

In the limiting case when $\gamma = 1$ we will get the expression (16) for the magnetized particle motion around Schwarzschild BH in the magnetic field (see, e.g., [73]). Consider the conditions

$$\dot{r} = 0, \quad \frac{\partial V_{\text{eff}}}{\partial r} = 0, \quad (20)$$

which define the circular orbits of the magnetized particles around the compact gravitational object. The solution of the first equation in (20) with respect to the coupling parameter β has the following form

$$\beta(r, l, \mathcal{E}, \gamma) = \frac{1}{\mathcal{L}[\lambda_{\hat{a}}]} \left(1 + f^{\gamma-1} \frac{l^2}{r^2} - \frac{\mathcal{E}^2}{f^\gamma} \right). \quad (21)$$

Using the expression (16) one can easily rewrite the second condition in (20) in the following form

$$\frac{\partial V_{\text{eff}}}{\partial r} = f^\gamma \mathcal{L}[\lambda_{\hat{a}}] \frac{\partial \beta}{\partial r}. \quad (22)$$

Now one can easily find the explicit form of the magnetic interaction term between the magnetic field and particle's magnetic moment in the following form

$$D^{\alpha\beta}F_{\alpha\beta} = 2\mu B f^\gamma e^\Psi, \quad (23)$$

where $e^\Psi = [f^\gamma - \Omega^2 r^2]^{-\frac{1}{2}}$ and Ω is the angular velocity of the particle at the equatorial plane.

Comparison of Equations (23) and (11) gives us the following relation

$$\mathcal{L}[\lambda_{\hat{a}}] = e^\Psi f^\gamma. \quad (24)$$

The angular velocity of the magnetized particle can be found as

$$\Omega = \frac{d\phi}{dt} = \frac{d\phi/d\tau}{dt/d\tau} = \frac{f^{2\gamma-1} l}{r^2 \mathcal{E}}. \quad (25)$$

Finally, one may obtain the following expression for the magnetic coupling parameter $\beta(r, l, \mathcal{E}, \gamma)$

$$\beta(r, l, \mathcal{E}, \gamma) = \left[\frac{1}{f^\gamma} - \left(\frac{f^{1-\gamma} l}{r \mathcal{E}} \right)^2 \right]^{\frac{1}{2}} \left(1 + f^{1-\gamma} \frac{l^2}{r^2} - \frac{\mathcal{E}^2}{f^\gamma} \right). \quad (26)$$

Figure 2 illustrates the radial dependence of the β function for the different values of γ -parameter and angular momentum.

The condition for existence of the stable circular orbits for the magnetized particles can be expressed using the β function as

$$\beta = \beta(r; l, \mathcal{E}, \gamma), \quad \frac{\partial \beta(r; l, \mathcal{E}, \gamma)}{\partial r} = 0, \quad (27)$$

which is the system of two equations with five parameters $\beta, r, l, \mathcal{E}, \gamma$. The solution of Equation (27) can be parametrized in terms of any two of four independent variables. We will use the radius and the magnetic coupling parameter as free parameters. One may find the minimum value of the specific angular momentum l and energy \mathcal{E} of the magnetized particle as function of coupling parameter β and radius of the circular orbits r as a free parameter for the different values of γ -parameter. The minimum value of the energy of the magnetized particles at stable circular orbits will have the following form

$$\mathcal{E}_{\min}^2(r; l, \gamma) = \frac{l^2 f[r + (\gamma - 3)M]}{\gamma M r^2}. \quad (28)$$

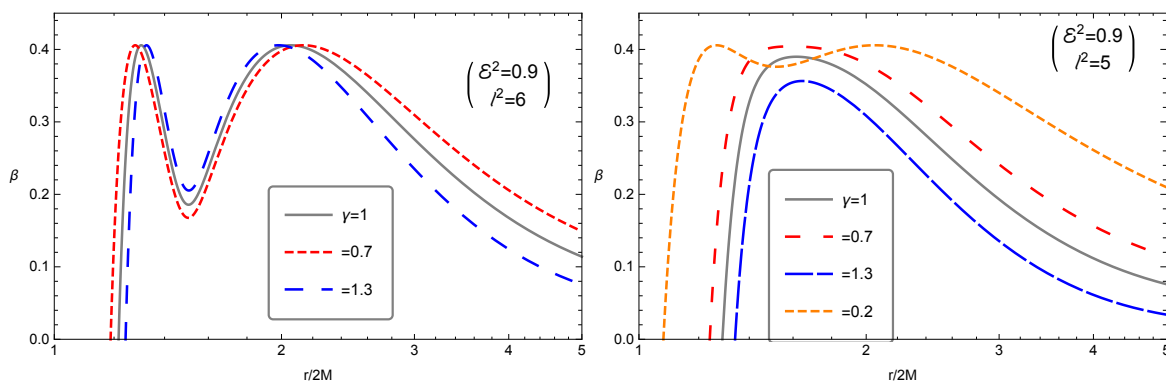


Figure 2. The radial dependence of the magnetic coupling parameter for the different values of γ -parameter. The plots are shown for the different values of the specific angular momentum: $l^2 = 6$ (left panel) and $l^2 = 5$ (right panel) when $\mathcal{E}^2 = 0.9$.

Figure 3 shows the radial dependence of the minimum value of the specific energy of magnetized particles at stable circular orbits for the different values of γ -parameter and for the fixed value of angular momentum ($l^2 = 5$). From the obtained dependence one can see that the energy is the same for all values of the γ -parameter at $r = 3M$ and has the value $\mathcal{E}_{\min} = l/(3\sqrt{3})$. However, at the distances $r > 3M$ the energy decreases with the increase of the γ -parameter. Inserting Equation (28) into Equation (26) one can calculate the minimum value of the β parameter as

$$\beta_{\min}(r; l, \gamma) = \frac{1}{f^{\frac{3\gamma}{2}} \gamma M r^3} \left\{ \gamma M r^3 f^\gamma + l^2 \left[M r [\gamma(f-1) + 5] + 2(\gamma-3)M^2 - r^2 \right] \right\} \quad (29)$$

$$\times \sqrt{1 + \frac{\gamma f M r}{(2M-r)[(\gamma-3)M+r]}}$$

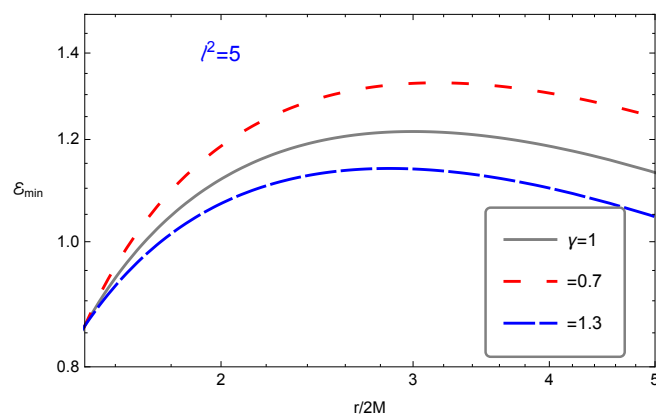


Figure 3. The radial dependence of the minimum value of specific energy of the magnetized particles for the different fixed values of γ -parameter.

Figure 4 demonstrates the radial dependence of extreme and minimum values of the β parameter at $l = 0$. The colored area indicates the set of values for β parameter and distances that correspond to stable circular orbits near position $r = 3M$. From Figure 4, one can see that the allowed range Δr for orbits shrinks (expands) with the decrease (increase) of γ -parameter.

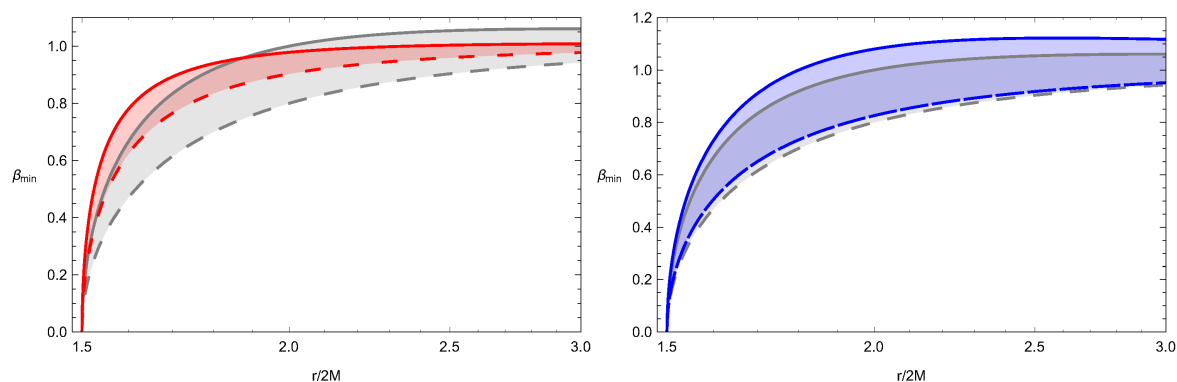


Figure 4. The radial dependence of the minimum values of the magnetic coupling parameter for the different fixed values of γ -parameter. The values of the particle specific energy and angular momentum are taken as $\mathcal{E}^2 = 0.9$ and $l^2 = 5$, respectively. In the left panel the red colored dashed and solid lines correspond to the case $\gamma = 0.4$. In the right panel the blue dashed and solid lines correspond to the case $\gamma = 1.6$. The grey lines correspond to the Schwarzschild case $\gamma = 1$.

The minimum value of the specific angular momentum can be found by solving the equation $\partial\beta_{\min}/\partial r = 0$ with respect to the specific angular momentum l^2 as

$$l_{\min}^2(r; \gamma) = \frac{\gamma^2 M^2 r^3 f^\gamma}{(r - 2M)(r - 3M)[2r + 3(\gamma - 2)M]} . \quad (30)$$

Figure 5 shows the radial dependence of the minimum value of specific angular momentum corresponding to the stable circular orbits for the different values of γ -parameter. One can see from the results of Figure 5 that the value of the specific angular momentum tends to infinity at $r = 3M$ and decreases with the increase of radial coordinate ($r \geq 3M$) as a power-law function. Furthermore, the degree of the power decreases with the increase of the parameter γ . Physically this implies the fact that in the case when parameter $\gamma < 1$ ($\gamma > 1$), gravitational interaction of the central object becomes weaker (stronger).

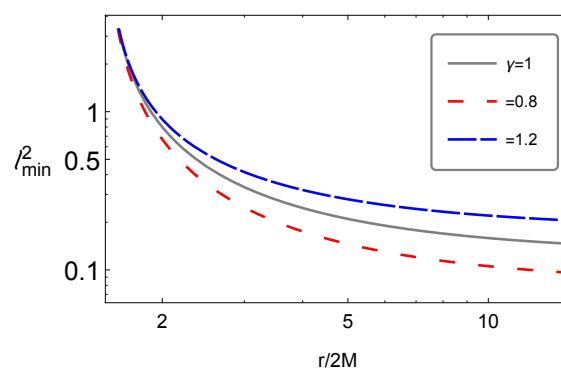


Figure 5. Radial dependence of minimum values of specific angular momentum for the different fixed values of γ -parameter.

Now we will substitute the expression for minimum value of the specific angular momentum (30) into Equation (29) and get

$$\beta_{\text{extr}}(r; \gamma) = \frac{2}{f^{\frac{\gamma}{2}}} \frac{\sqrt{(r - 3M)[r + (\gamma - 3)M]}}{2r + 3(\gamma - 2)M} . \quad (31)$$

The effect of γ -parameter on the extreme value of the magnetic coupling parameter corresponding to the upper limit of stable circular orbits for magnetized particles is presented in Figure 6. One can easily see from Figure 6 that the extreme value of the β parameter increases for $\gamma \neq 1$. It is due to strong influence of γ -parameter on the magnetic field structure (see [34] for more details). In Figure 6, blue dashed and red dashed lines correspond to $\gamma = 1.7$ and $\gamma = 0.3$, respectively.

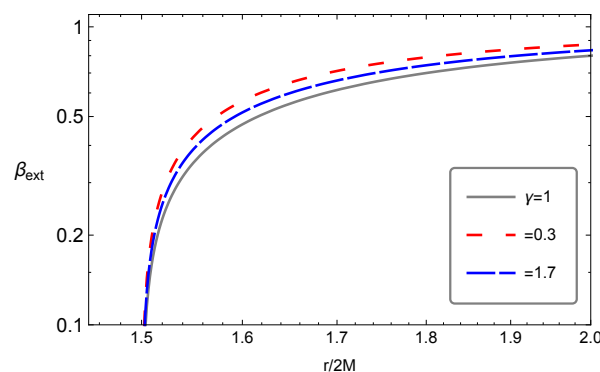


Figure 6. Radial dependence of the extreme value of the magnetic coupling parameter β for the different selected values of the parameter γ .

Analysis of the expressions for minimum and extreme values of the magnetic coupling parameter β show that both $\beta_{\text{ext}} = \beta_{\text{min}} = 0$ at $r \leq 3M$ (see Figures 4 and 6). It implies that no magnetized particle can be at stable circular orbit inside the distance $3M$ from the central object. This fundamental result does not depend on the value of the parameter γ .

Solving the equation $\beta = \beta_{\text{min}}$ with respect to l one may rewrite the expressions for the minimum value of specific angular momentum in terms of parameter β in the following form

$$l_{\text{min}}^2(r, \gamma, \beta) = \frac{\gamma M r^3 f^\gamma}{(r-2M)(r-3M)} \left[1 - f^{\frac{\gamma}{2}} \sqrt{\frac{r-(3-\gamma)M}{r-3M}} \beta \right]. \quad (32)$$

Substituting Equation (32) in to Equation (28) one can get

$$\mathcal{E}_{\text{min}}^2(r, \gamma, \beta) = \frac{f^\gamma (r + (3-\gamma)M)}{(r-3M)^3} \left[f^{\frac{\gamma}{2}} \sqrt{\frac{r-(3-\gamma)M}{r-3M}} \beta - 1 \right].$$

One may now consider the range of stable circular orbits of the magnetized particles around the gravitational γ object immersed in the magnetic field for different values of the parameter γ . It is obvious that the value of stable orbits radius $r = r_{\text{min}}$ takes the minimum value at $l = 0$ (in this case the repulsive Lorentz force compensates an attractive gravitational one) for minimum specific energy. It can be found through the solution of the following equation

$$\beta = \beta_{\text{min}}(r, \gamma, l = 0). \quad (33)$$

The upper limit for stable orbits can be found using the condition when centrifugal and Lorentz forces are balanced with the gravitational force. In other words, the value of angular momentum can not exceed the value l_{min} and the value of the function β corresponds to the upper limit for the magnetic coupling parameter. The maximum radius of the orbits r_{max} can be found by solving the following equation

$$\beta = \beta_{\text{extr}}(r, \gamma). \quad (34)$$

The range between r_{min} and r_{max} is the area where stable orbits for magnetized particles are allowed. The numerical solutions of Equations (33) and (34) are presented in Table 1. From the results in Table 1 one can see that the range $\Delta r = r_{\text{max}} - r_{\text{min}}$ increases with the increase of both β and γ -parameters. For the case $\beta \geq 1$ there are no circular orbits. The circular orbits may exist at spatial infinity because the limits of both extreme and minimum values of the β parameter at $l = 0$ have the following values

$$\lim_{r \rightarrow \infty} \beta_{\text{min}}(r, \gamma, l = 0) = 1, \quad \lim_{r \rightarrow \infty} \beta_{\text{extr}}(r, \gamma) = 1. \quad (35)$$

Using the above estimation in Equation (18) one may conclude that a magnetar with the dipole magnetic field $B_{\text{NS}} \geq 5 \times 10^{14}$ G cannot be in circular orbits in the close environment of Sgr A*.

Table 1. Numerical values for $\Delta r = r_{\text{max}} - r_{\text{min}}$ for the different values of the magnetic coupling parameter β and the parameter γ . Units of the Δr are given in mass M .

β	$\gamma = 0.5$	$\gamma = 0.7$	$\gamma = 0.9$	$\gamma = 1$	$\gamma = 1.2$	$\gamma = 1.25$
0.2	0.01481	0.01672	0.01683	0.01729	0.01694	0.01649
0.5	0.10969	0.11562	0.126684	0.13488	0.13247	0.13112
0.7	0.28643	0.337	0.350061	0.37412	0.37139	0.36907
0.9	1.02217	1.22498	1.35529	1.39532	1.4275	1.42591
0.99	6.33322	7.37185	8.01438	8.20703	8.35397	8.34246

3. Astrophysical Applications

The study and analysis of the observed data on the electromagnetic spectra of BH's accretion disk may be helpful to investigate the geometry of the spacetime around the central object and construct new tests of extended theories of gravity in a strong field regime. Particularly, observations of micro-quasars (BH binaries) can help to study the inner edge of an accretion disk corresponding to ISCO and get estimations for parameters of the BH such as spin parameter of Kerr BH. However, the central object may not be described exactly by the Kerr geometry but by other exact solutions of extended theories of gravity, which may mimic the observational features of astrophysical BH. In this section we will focus on showing how the magnetic coupling and γ -parameters can mimic the spin of rotating Kerr BH, providing exactly the same value for the ISCO radius of magnetized particles. Note that one may consider magnetized particles as neutral test particles in the study of their dynamics around rotating Kerr BHs in a vacuum.

Here we consider the astrophysical applications of the theoretical study of the ISCO of neutral particles around the compact object in γ -spacetime. We compare our results with the ISCO radius of test particles around rapidly rotating Kerr BH with non-vanishing spin parameter a .

The ISCO radius of the test particles around rotating Kerr BH can be expressed as [96]

$$r_{\text{isco}} = 3 + Z_2 \pm \sqrt{(3 - Z_1)(3 + Z_1 + 2Z_2)}, \quad (36)$$

where

$$\begin{aligned} Z_1 &= 1 + \left(\sqrt[3]{1-a} + \sqrt[3]{1+a} \right) \sqrt[3]{1-a^2}, \\ Z_2^2 &= 3a^2 + Z_1^2. \end{aligned} \quad (37)$$

Note that in Equation (36) and in the notation used, all parameters are normalized to the BH mass M , '-' ('+') sign corresponds to pro-grate (retro-grate) orbits of particles around Kerr BH.

In this application our aim is to investigate the ISCO radius of magnetized particles around (i) Schwarzschild BH in the magnetic field, (ii) Kerr BH and (iii) deformed γ -spacetime in the magnetic field in order to get degenerate values of spin, magnetic coupling and γ -parameters giving the same ISCO radius.

Figure 7 demonstrates the dependence of the ISCO radius of the magnetized particle from magnetized coupling, rotation and γ -parameters. One can see that γ -parameter can mimic the spin of Kerr BH on the observations of ISCO radii of test particles. One can also conclude that the possibility of distinguishing the Kerr BH from the other gravitational objects mentioned above for the values of spin parameter $a \geq 0.85$ if only the ISCO radius of the particle is approximately $r_{\text{isco}} \leq 2.2M$ (see Figure 7).

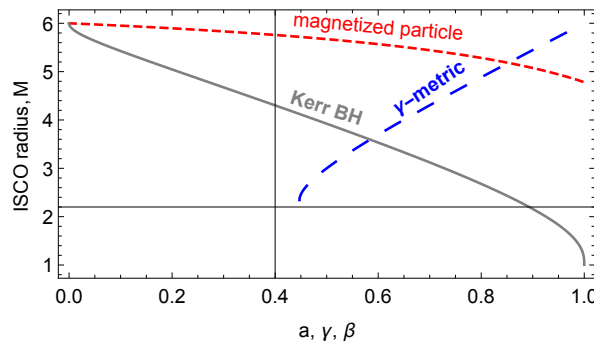


Figure 7. The dependence of the innermost stable circular orbit (ISCO) radius from the dimensionless rotation parameter a , γ -parameter and magnetic coupling parameter β .

Now, we will give a detailed analysis of the mimicker degeneracy cases between rotation, γ -and magnetic coupling parameters.

In Figure 8 we present the relations between (i) γ and rotation a parameters (red colored dashed line), (ii) γ and magnetic coupling β parameters (blue colored large dashed line), rotation a and magnetic coupling β parameters (gray colored solid line) providing the same values of the ISCO radius.

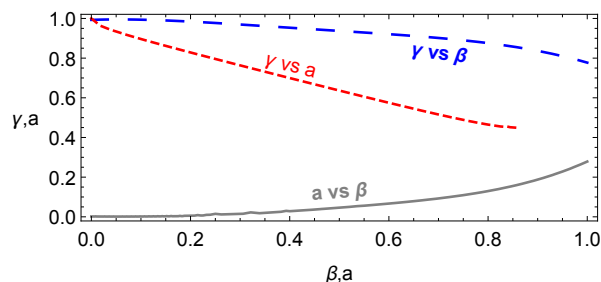


Figure 8. Degeneracy relation between the parameters β and γ corresponding to the same ISCO radius of magnetized particles.

Results show the following degeneracy values of the parameters:

- (i) The study of the ISCO radius of a test magnetized particles around rotating Kerr BH and deformed spacetime of γ -object shows the degeneracy relation between the rotation parameter a and γ -parameter corresponding to exactly the same value of the ISCO radius of the magnetized particles. One can see from the red dashed line in Figure 8 that the rotation parameter a of the Kerr BH can be mimicked by the effect of the γ -parameter for the range $\gamma \in (0.5, 1)$ providing the same ISCO radius.
- (ii) In the case of magnetized particles motion around the BH immersed in the magnetic field and the deformed static object described by γ -metric, the same ISCO radius for the magnetized particles can be observed. The detailed analysis shows that (see red dashed line in Figure 8) γ -parameter in the range of values of $\gamma \in (0.8, 1)$ can mimic the magnetic coupling parameter up to $\beta = 1$ providing the same ISCO radius.
- (iii) The external magnetic field can mimic the rotation parameter of the Kerr BH through astronomical observations of the motion of magnetized particles around Schwarzschild BH immersed in an external asymptotically-uniform magnetic field providing exactly the same values of the ISCO radius. One can see from Figure 8 (blue large dashed line) that the values of the magnetic coupling parameter $\beta \leq 1$ can mimic the spin of rotating Kerr BH up to $a \simeq 0.3$.

4. Magnetized Particles Acceleration in γ -Spacetime

In this section, we will study the center-of-mass energy of two colliding particles. We will consider the magnetized-magnetized, magnetized-neutral, and magnetized-charged particles collisions. The expression for the center-of-mass energy for two particles can be found as the sum of two-momenta [93,97,98]

$$\{E_{cm}, 0, 0, 0\} = m_1 u_1^\mu + m_2 u_2^\mu, \quad (38)$$

where, u_1^α and u_2^β are the four-velocities of the two colliding particles with the masses m_1 and m_2 , respectively. One can easily calculate the square of center-of-mass energy defined in (38) and get

$$E_{cm}^2 = m_1^2 + m_2^2 - 2m_1 m_2 g_{\mu\nu} u_1^\mu u_2^\nu, \quad (39)$$

or

$$\frac{E_{cm}^2}{m_1 m_2} = \frac{m_1}{m_2} + \frac{m_2}{m_1} - 2g_{\mu\nu} u_1^\mu u_2^\nu. \quad (40)$$

Hereafter, we will consider the collision of the particles with the equal mass $m_1 = m_2 = m$ and initial energy as $E_1 = E_2 = m$. Then the expression for the center-of-mass energy takes a different form depending on colliding particles.

4.1. Collision of Two Magnetized Particles

Using the equations of motion for magnetized particles (12)–(14) one may easily calculate the specific center-of-mass energy ($\mathcal{E}_{cm} = E_{cm}/(mc^2)$) of colliding two magnetized particles in the following form

$$\begin{aligned} \mathcal{E}_{cm}^2 &= 1 + \frac{\mathcal{E}_1 \mathcal{E}_2}{f^\gamma} - f^{2(\gamma-1)} \frac{l_2 l_1}{r^2} - \sqrt{\mathcal{E}_1^2 - \left(1 + f^{2\gamma-1} \frac{l_1^2}{r^2} - \beta_1 f^\gamma\right)} \\ &\times \sqrt{\mathcal{E}_2^2 - \left(1 + f^{2\gamma-1} \frac{l_2^2}{r^2} - \beta_2 f^\gamma\right)}. \end{aligned} \quad (41)$$

In Figure 9 we show the radial dependence of the center-of-mass energy of two colliding magnetized particles near the compact γ -object in the presence of an external asymptotically uniform magnetic field. One can see from Figure 9 that the center-of-mass energy increases with the increase of γ -parameter due to the increase of gravitational potential.

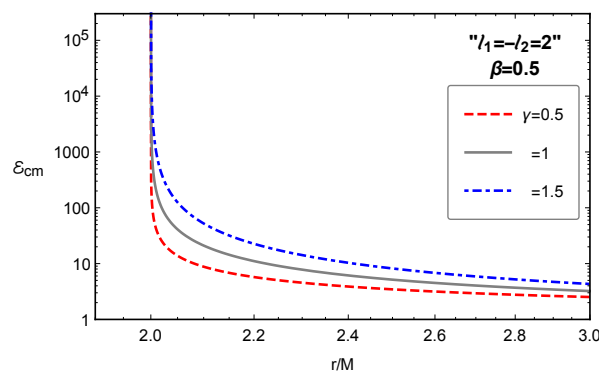


Figure 9. Radial dependence of center-of-mass energy of two colliding magnetized particles. The plots have been taken for the values of initial energy $\mathcal{E}_1 = \mathcal{E}_2 = 1$ and specific angular momentum $l_1 = -l_2 = 2M$ of the colliding particles.

4.2. Collision of Magnetized and Charged Particles

In this subsection, we consider the collision of a magnetized particle with a charged one. The four-velocity of the charged particle can be found using the Lagrangian for the charged particle in curved spacetime in the presence of an electromagnetic field that has the following form

$$\mathcal{L} = \frac{1}{2} m g_{\mu\nu} u^\mu u^\nu + e u^\mu A_\mu, \quad (42)$$

where m , e , and $u^\alpha (= dx^\alpha/d\tau)$ are the rest mass, the electric charge, and the four-velocity of the particle, respectively. The energy and the angular momentum can be found by

$$p_t = \frac{\partial \mathcal{L}}{\partial \dot{t}} \rightarrow -E = m g_{tt} u^t, \quad (43)$$

$$p_\phi = \frac{\partial \mathcal{L}}{\partial \dot{\phi}} \rightarrow L = m g_{\phi\phi} u^\phi + e A_\phi, \quad (44)$$

and the components of four-velocity of the charged particle take the following form

$$\begin{aligned} \dot{t} &= \frac{\mathcal{E}}{f^\gamma}, \\ f^{\gamma^2-1} \dot{r}^2 &= \mathcal{E}^2 - f^{2\gamma-1} \left[1 + \left(\frac{l}{r} - \omega_B r f^{1-\gamma} \right)^2 \right], \\ \dot{\phi} &= f^{\gamma-1} \frac{l}{r^2} - \omega_B, \end{aligned} \quad (45)$$

where $\omega_B = eB/(2mc)$ is the cyclotron frequency of the charged particle in the uniform magnetic field B .

The expression for center-of-mass energy of colliding magnetized and charged particles takes the form

$$\begin{aligned} \mathcal{E}_{cm}^2 &= 1 + \frac{\mathcal{E}_1 \mathcal{E}_2}{f^\gamma} - f^{\gamma-1} l_1 \left(f^{\gamma-1} \frac{l_2}{r^2} - \omega_B \right) - \sqrt{\mathcal{E}_2^2 - \left(1 + f^{2\gamma-1} \frac{l_2^2}{r^2} - \beta f^\gamma \right)} \\ &\times \sqrt{f^{1-\gamma^2} \left\{ \mathcal{E}_1^2 - f^{2\gamma-1} \left[1 + \left(\frac{l_1}{r} - \omega_B r f^{1-\gamma} \right)^2 \right] \right\}}. \end{aligned} \quad (46)$$

In Figure 10 we show the radial dependence of the center-of-mass energy of collision of magnetized and charged particles near the compact γ -object in the presence of an external asymptotically uniform magnetic field. One can see that in the case of the collision of magnetized and positively charged particles the inner and outer collision points match to the area of stable circular orbits corresponding to the values of angular momentum $l = 2M$ and parameter $\gamma = 1.5$. However, in the cases of $\gamma = 1$ and $\gamma = 0.5$ the inner position of the collisions comes close to the infinitely red-shifted surface $r = 2M$. In the case of both positively and negatively charged particles with magnetized particles, the particle collisions do take place at far distances from the compact object due to the Lorentz force. The Lorentz force becomes dominant at far distances and the magnetic field forces the charged particles to escape to infinity. Moreover, one can see that the maximum value of the center-of-mass energy decreases in the presence of both types of deformation cases corresponding to $\gamma > 1$ and $\gamma < 1$ due to the effect of γ -parameter on the external magnetic field near the BH (see [34] for the details).

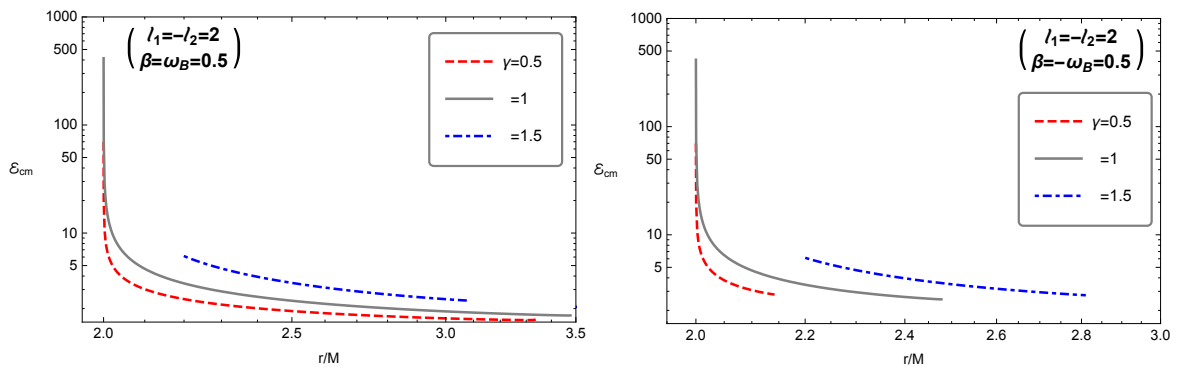


Figure 10. The same figure as Figure 9, but for the collision of charged and magnetized particles. Left and right panels correspond to the collision of the magnetized particle with positively and negatively charged particles, respectively. In these plots we have taken the same values for the interaction parameters of charged and magnetized particles $\beta = \omega_B = 0.5$.

4.3. Collision of Magnetized and Neutral Particles

In this subsection, we investigate the collision of magnetized and neutral particles. The equation of motion for neutral particles can be written as follows

$$\begin{aligned} \dot{t} &= \frac{\mathcal{E}}{f^2}, \\ \dot{r}^2 &= \mathcal{E}^2 - f^{2\gamma-1} \left(1 + \frac{l^2}{r^2} \right), \\ \dot{\phi} &= f^{\gamma-1} \frac{l}{r^2}. \end{aligned} \quad (47)$$

The expression for center-of-mass energy of colliding magnetized and neutral particles takes the following form

$$\begin{aligned} \mathcal{E}_{cm}^2 &= 1 + \frac{\mathcal{E}_1 \mathcal{E}_2}{f^\gamma} - f^\gamma \frac{l_2 l_1}{r^2} - \sqrt{f^{1-\gamma^2} \left[\mathcal{E}_1^2 - f^{2\gamma-1} \left(1 + \frac{l_1^2}{r^2} \right) \right]} \\ &\times \sqrt{\mathcal{E}_2^2 - \left(1 + f^{2\gamma-1} \frac{l_2^2}{r^2} - \beta f^\gamma \right)}. \end{aligned} \quad (48)$$

In Figure 11, we show the radial dependence of the center-of-mass energy of the collision of magnetized and neutral particles near the γ -compact object in the presence of an external asymptotically uniform magnetic field. One can see from Figure 11 that the center-of-mass energy increases with the increase of the value of γ -parameter. However, the maximum value of the energy decreases in both cases when $\gamma > 1$ and $\gamma < 1$. Moreover, the collisions take place near the infinitely red-shifted surface $r = 2M$, and at large distances, the Lorentz force causes the magnetized particles to escape to infinity.

In Figure 12, we have shown the relation of γ -parameter and the magnetized coupling parameter causing the increase of the center-of-mass energy to the values exceeding $10^6 mc^2$ at the distance $r = 3M$ (indicated with shaded area). The analysis shows that it requires large values of β parameter.

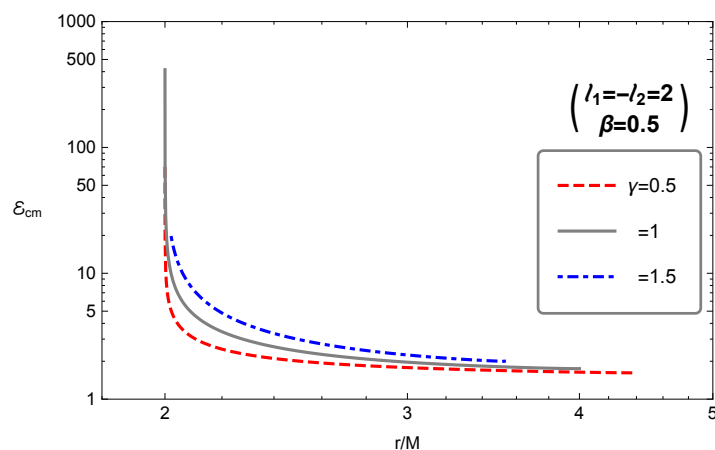


Figure 11. The same figure as Figure 9, but for the collision of magnetized and neutral particles.

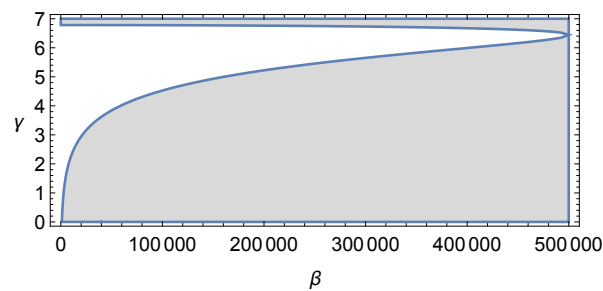


Figure 12. Dependence between magnetic coupling parameter β and γ -parameter for the values of center-of-mass energy of two colliding magnetized particles exceeding $\mathcal{E} > 10^6$ at the distance $r = 3M$ when angular momentum $l_1 = -l_2 = 2M$.

5. Summary and Discussions

In this work, we have investigated the dynamics of the magnetized particles and energetic processes, namely the acceleration process during the collision of magnetized and charged particles in close vicinity of the compact γ -object immersed in an external asymptotically-uniform magnetic field. One of the aims of this note is the motion of a highly magnetized neutron star treated as the test magnetized particle around the supermassive BH (SMBH). The neutron star treated as the magnetized test particle can interact with the magnetic field in SMBH environment, which causes to change of the characteristic radii, namely the ISCO radius of the magnetized neutron star in the SMBH environment. Due to this fact and its compactness, which decreases the tidal forces, the magnetized neutron star can orbit very near to the SMBH in comparison with observed S stars observed in infrared (IR) wavelength. The main results of the paper can be summarized as follows:

- We have analyzed the magnetic coupling parameter being responsible for circular stable orbits at the given specific angular momentum and specific energy. It has been shown that the maximum value of the magnetic coupling parameter β does not depend on the value of γ -parameter. It is due to the fact that the Lorentz force dominates at the maximum values of the magnetic interaction parameter. Consequently, it is not sensitive to any value of γ -parameter.
- It has also been shown that the minimum value of the specific energy corresponding to stable circular orbits of magnetized particles decreases with the increase of the value of γ -parameter due to the decreasing of the gravitational potential at $\gamma > 1$.
- It has been obtained that the minimum value of the specific angular momentum corresponding to the extreme value of the magnetic coupling parameter causes a decrease in the distance between the innermost and outermost stable circular orbits. The magnetized particle's circular orbits can not be stable ones for the values $\beta > 1$. This may be helpful to predict that no magnetized neutron star can be observed in circular orbits in an environment of Sgr A* when the dipole magnetic field is greater than 5×10^{14} Gauss.
- We have studied the acceleration process in the collision of magnetized particles around compact objects in γ -spacetime. We have shown that the center-of-mass energy of collision of magnetized particles increases with the increase of the γ -parameter.
- Finally, we have applied the obtained results to the real astrophysical scenario and shown distinguishable features of the three different geometries. Particularly, analyzing the ISCO radii of magnetized particles around Kerr, deformed γ -spacetime and Schwarzschild BH immersed in an asymptotically-uniform magnetic field. We have shown that the γ -parameter can mimic the spin parameter of Kerr BH $a \leq 0.85$, while the magnetic coupling parameter $\beta < 1$ can mimic the γ -parameter for the range (0.5, 1) and the rotation parameter of Kerr BH $a \leq 0.3$.

Author Contributions: Conceptualization, A.A., J.R. and B.A.; methodology, J.R.; software, F.A., J.R.; validation, B.A., A.A. and F.A.; formal analysis, F.A., A.A.; investigation, F.A., A.A., J.R., B.A. All authors have read and agreed to the published version of the manuscript.

Funding: This research is supported by Grants No. VA-FA-F-2-008 and No. MRB-AN-2019-29 of the Uzbekistan Ministry for Innovative Development. A.A. was funded by the PIFI fund of the Chinese Academy of Sciences.

Acknowledgments: The authors thank the Silesian University in Opava for hospitality.

Conflicts of Interest: The authors declare no conflict of interest.

References

- Wald, R.M. Black hole in a uniform magnetic field. *Phys. Rev. D* **1974**, *10*, 1680–1685. [[CrossRef](#)]
- Aliev, A.N.; Özdemir, N. Motion of charged particles around a rotating black hole in a magnetic field. *Mon. Not. R. Astron. Soc.* **2002**, *336*, 241–248. [[CrossRef](#)]
- Frolov, V.P.; Shoom, A.A. Motion of charged particles near a weakly magnetized Schwarzschild black hole. *Phys. Rev. D* **2010**, *82*, 084034. [[CrossRef](#)]
- Abdujabbarov, A.; Ahmedov, B. Test particle motion around a black hole in a braneworld. *Phys. Rev. D* **2010**, *81*, 044022. [[CrossRef](#)]
- Abdujabbarov, A.; Ahmedov, B.; Hakimov, A. Particle motion around black hole in Hořava-Lifshitz gravity. *Phys. Rev. D* **2011**, *83*, 044053. [[CrossRef](#)]
- Frolov, V.P. Weakly magnetized black holes as particle accelerators. *Phys. Rev. D* **2012**, *85*, 024020. [[CrossRef](#)]
- Karas, V.; Kovar, J.; Kopacek, O.; Kojima, Y.; Slany, P.; Stuchlík, Z. Regular and Chaotic Motion in General Relativity. Case of Magnetized Black Hole and a Massive Magnetic Dipole. *Am. Astron. Soc. Meet. Abstr.* **2012**, *220*, 430-07.
- Hakimov, A.; Abdujabbarov, A.; Ahmedov, B. Magnetic fields of spherical compact stars in modified theories of gravity: $f(R)$ type gravity and Hořava-Lifshitz gravity. *Phys. Rev. D* **2013**, *88*, 024008. [[CrossRef](#)]
- Stuchlík, Z.; Schee, J.; Abdujabbarov, A. Ultra-high-energy collisions of particles in the field of near-extreme Kehagias-Sfetsos naked singularities and their appearance to distant observers. *Phys. Rev. D* **2014**, *89*, 104048. [[CrossRef](#)]
- Stuchlík, Z.; Kološ, M. Acceleration of the charged particles due to chaotic scattering in the combined black hole gravitational field and asymptotically uniform magnetic field. *Eur. Phys. J. C* **2016**, *76*, 32. [[CrossRef](#)]
- Turimov, B.V.; Ahmedov, B.J.; Abdujabbarov, A.A. Electromagnetic Fields of Slowly Rotating Magnetized Gravastars. *Mod. Phys. Lett. A* **2009**, *24*, 733–737. [[CrossRef](#)]
- Rayimbaev, J.R.; Ahmedov, B.J.; Juraeva, N.B.; Rakhmatov, A.S. Plasma magnetosphere of deformed magnetized neutron star. *Astrophys. Space Sci.* **2015**, *356*, 301–308. [[CrossRef](#)]
- Turimov, B.V.; Ahmedov, B.J.; Hakimov, A.A. Stationary electromagnetic fields of slowly rotating relativistic magnetized star in the braneworld. *Phys. Rev. D* **2017**, *96*, 104001. [[CrossRef](#)]
- Rayimbaev, J.; Turimov, B.; Ahmedov, B. Braneworld effects in plasma magnetosphere of a slowly rotating magnetized neutron star. *Int. J. Mod. Phys. D* **2019**, *28*, 1950128. [[CrossRef](#)]
- Rayimbaev, J.; Turimov, B.; Palvanov, S. Plasma magnetosphere of slowly rotating magnetized neutron star in braneworld. *Int. J. Mod. Phys. Conf. Ser.* **2019**, *49*, 1960019. [[CrossRef](#)]
- Rayimbaev, J.; Tadjimuratov, P. Can modified gravity silence radio-loud pulsars? *Phys. Rev. D* **2020**, *102*, 024019. [[CrossRef](#)]
- Turimov, B.; Ahmedov, B.; Abdujabbarov, A.; Bambi, C. Electromagnetic fields of slowly rotating magnetized compact stars in conformal gravity. *Phys. Rev. D* **2018**, *97*, 124005. [[CrossRef](#)]
- Turimov, B. Electromagnetic fields in vicinity of tidal charged static black hole. *Int. J. Mod. Phys. D* **2018**, *27*, 1850092. [[CrossRef](#)]
- Rayimbaev, J.; Turimov, B.; Marcos, F.; Palvanov, S.; Rakhmatov, A. Particle acceleration and electromagnetic field of deformed neutron stars. *Mod. Phys. Lett. A* **2020**, *35*, 2050056. [[CrossRef](#)]
- Penrose, R. Solutions of the Zero-Rest-Mass Equations. *J. Math. Phys.* **1969**, *10*, 38–39. [[CrossRef](#)]
- Blandford, R.D.; Znajek, R.L. Electromagnetic extraction of energy from Kerr black holes. *Mon. Not. R. Astron. Soc.* **1977**, *179*, 433–456. [[CrossRef](#)]
- Dhurandhar, S.V.; Dadhich, N. Energy extraction processes near a Kerr black hole immersed in a magnetic field. *Bull. Astron. Soc. India* **1983**, *11*, 85.

23. Dhurandhar, S.V.; Dadhich, N. Energy-extraction processes from a Kerr black hole immersed in a magnetic field. I. Negative-energy states. *Phys. Rev. D* **1984**, *29*, 2712–2720. [[CrossRef](#)]
24. Dhurandhar, S.V.; Dadhich, N. Energy-extraction processes from a Kerr black hole immersed in a magnetic field. II. The formalism. *Phys. Rev. D* **1984**, *30*, 1625–1631. [[CrossRef](#)]
25. Wagh, S.M.; Dhurandhar, S.V.; Dadhich, N. Revival of the Penrose process for astrophysical applications. *Astrophys. J.* **1985**, *290*, 12–14. [[CrossRef](#)]
26. Bañados, M.; Silk, J.; West, S.M. Kerr Black Holes as Particle Accelerators to Arbitrarily High Energy. *Phys. Rev. Lett.* **2009**, *103*, 111102. [[CrossRef](#)]
27. Abdujabbarov, A.A.; Ahmedov, B.J.; Kagramanova, V.G. Particle motion and electromagnetic fields of rotating compact gravitating objects with gravitomagnetic charge. *Gen. Relativ. Gravit.* **2008**, *40*, 2515–2532. [[CrossRef](#)]
28. Abdujabbarov, A.A.; Tursunov, A.A.; Ahmedov, B.J.; Kuvatov, A. Acceleration of particles by black hole with gravitomagnetic charge immersed in magnetic field. *Astrophys. Space Sci.* **2013**, *343*, 173–179. [[CrossRef](#)]
29. Abdujabbarov, A.A.; Ahmedov, B.J.; Jurayeva, N.B. Charged-particle motion around a rotating non-Kerr black hole immersed in a uniform magnetic field. *Phys. Rev. D* **2013**, *87*, 064042. [[CrossRef](#)]
30. Abdujabbarov, A.; Ahmedov, B.; Rahimov, O.; Salikhbaev, U. Magnetized particle motion and acceleration around a Schwarzschild black hole in a magnetic field. *Phys. Scr.* **2014**, *89*, 084008. [[CrossRef](#)]
31. Narzilloev, B.; Rayimbaev, J.; Shaymatov, S.; Abdujabbarov, A.; Ahmedov, B.; Bambi, C. Can the dynamics of test particles around charged stringy black holes mimic the spin of Kerr black holes? *Phys. Rev. D* **2020**, *102*, 044013. [[CrossRef](#)]
32. Narzilloev, B.; Abdujabbarov, A.; Bambi, C.; Ahmedov, B. Charged particle motion around a quasi-Kerr compact object immersed in an external magnetic field. *Phys. Rev. D* **2019**, *99*, 104009. [[CrossRef](#)]
33. Oteev, T.; Abdujabbarov, A.; Stuchlík, Z.; Ahmedov, B. Energy extraction and particle acceleration around a rotating black hole in quintessence. *Astrophys. Space Sci.* **2016**, *361*, 269. [[CrossRef](#)]
34. Benavides-Gallego, C.A.; Abdujabbarov, A.; Malafarina, D.; Ahmedov, B.; Bambi, C. Charged particle motion and electromagnetic field in γ spacetime. *Phys. Rev. D* **2019**, *99*, 044012. [[CrossRef](#)]
35. Benavides-Gallego, C.A.; Abdujabbarov, A.; Malafarina, D.; Bambi, C. Quasi-harmonic oscillations of charged particles in static axially symmetric space-times immersed in a uniform magnetic field. *Phys. Rev. D* **2020**, *101*, 124024. [[CrossRef](#)]
36. Tursunov, A.; Kološ, M.; Abdujabbarov, A.; Ahmedov, B.; Stuchlík, Z. Acceleration of particles in spacetimes of black string. *Phys. Rev. D* **2013**, *88*, 124001. [[CrossRef](#)]
37. Tursunov, A.; Stuchlík, Z.; Kološ, M. Circular orbits and related quasiharmonic oscillatory motion of charged particles around weakly magnetized rotating black holes. *Phys. Rev. D* **2016**, *93*, 084012. [[CrossRef](#)]
38. Kološ, M.; Stuchlík, Z.; Tursunov, A. Quasi-harmonic oscillatory motion of charged particles around a Schwarzschild black hole immersed in a uniform magnetic field. *Class. Quantum Gravity* **2015**, *32*, 165009. [[CrossRef](#)]
39. Kološ, M.; Tursunov, A.; Stuchlík, Z. Possible signature of magnetic fields related to quasi-periodic oscillation observed in microquasars. *Eur. Phys. J. C* **2017**, *77*, 860. [[CrossRef](#)]
40. Tursunov, A.A.; Kološ, M. Constraints on Mass, Spin and Magnetic Field of Microquasar H 1743–322 from Observations of QPOs. *Phys. At. Nucl.* **2018**, *81*, 279–282. [[CrossRef](#)]
41. Tursunov, A.; Kološ, M.; Stuchlík, Z.; Gal'tsov, D.V. Radiation Reaction of Charged Particles Orbiting a Magnetized Schwarzschild Black Hole. *Astrophys. J.* **2018**, *861*, 2. [[CrossRef](#)]
42. Shaymatov, S.; Ahmedov, B.; Stuchlík, Z.; Abdujabbarov, A. Effect of an external magnetic field on particle acceleration by a rotating black hole surrounded with quintessential energy. *Int. J. Mod. Phys. D* **2018**, *27*, 1850088. [[CrossRef](#)]
43. Shaymatov, S.; Malafarina, D.; Ahmedov, B. Effect of perfect fluid dark matter on particle motion around a static black hole immersed in an external magnetic field. *arXiv* **2020**, arXiv:2004.06811.
44. Kimura, M.; Nakao, K.I.; Tagoshi, H. Acceleration of colliding shells around a black hole: Validity of the test particle approximation in the Banados-Silk-West process. *Phys. Rev. D* **2011**, *83*, 044013. [[CrossRef](#)]
45. Zaslavskii, O.B. Energy extraction from extremal charged black holes due to the Banados-Silk-West effect. *Phys. Rev. D* **2012**, *86*, 124039. [[CrossRef](#)]

46. Bañados, M.; Hassanain, B.; Silk, J.; West, S.M. Emergent flux from particle collisions near a Kerr black hole. *Phys. Rev. D* **2011**, *83*, 023004. [[CrossRef](#)]
47. Shaymatov, S.; Atamurotov, F.; Ahmedov, B. Isofrequency pairing of circular orbits in Schwarzschild spacetime in the presence of magnetic field. *Astrophys. Space Sci.* **2014**, *350*, 413–419. [[CrossRef](#)]
48. Patil, M.; Hakimov, A.A.; Shaymatov, S.R. Particle acceleration in Kerr-TAUB-NUT naked singularities. *NEWS Natl. Acad. Sci. Repub. Kazakhstan* **2014**, *294*, 33–38.
49. Igata, T.; Harada, T.; Kimura, M. Effect of a weak electromagnetic field on particle acceleration by a rotating black hole. *Phys. Rev. D* **2012**, *85*, 104028. [[CrossRef](#)]
50. Toshmatov, B.; Abdujabbarov, A.; Ahmedov, B.; Stuchlík, Z. Motion and high energy collision of magnetized particles around a Hořava-Lifshitz black hole. *Astrophys. Space Sci.* **2015**, *360*, 19. [[CrossRef](#)]
51. Gao, S.; Zhong, C. Non-extremal Kerr black holes as particle accelerators. *Phys. Rev. D* **2011**, *84*, 044006. [[CrossRef](#)]
52. Liu, C.; Chen, S.; Ding, C.; Jing, J. Particle acceleration on the background of the Kerr-Taub-NUT spacetime. *Phys. Lett. B* **2011**, *701*, 285–290. [[CrossRef](#)]
53. Patil, M.; Joshi, P.S.; Malafarina, D. Naked singularities as particle accelerators. II. *Phys. Rev. D* **2011**, *83*, 064007. [[CrossRef](#)]
54. Patil, M.; Joshi, P.S.; Kimura, M.; Nakao, K.I. Acceleration of particles and shells by Reissner-Nordström naked singularities. *Phys. Rev. D* **2012**, *86*, 084023. [[CrossRef](#)]
55. Patil, M.; Joshi, P.S. Naked singularities as particle accelerators. *Phys. Rev. D* **2010**, *82*, 104049. [[CrossRef](#)]
56. Zaslavskii, O.B. Acceleration of particles by black holes: Kinematic explanation. *Phys. Rev. D* **2011**, *84*, 024007. [[CrossRef](#)]
57. Zaslavskii, O.B. Acceleration of particles by nonrotating charged black holes? *Sov. J. Exp. Theor. Phys. Lett.* **2010**, *92*, 571–574. [[CrossRef](#)]
58. Zaslavskii, O.B. Acceleration of particles by black holes—A general explanation. *Class. Quantum Gravity* **2011**, *28*, 105010. [[CrossRef](#)]
59. Ghosh, S.G.; Sheoran, P.; Amir, M. Rotating Ayón-Beato-García black hole as a particle accelerator. *Phys. Rev. D* **2014**, *90*, 103006. [[CrossRef](#)]
60. Shaymatov, S.R.; Ahmedov, B.J.; Abdujabbarov, A.A. Particle acceleration near a rotating black hole in a Randall-Sundrum brane with a cosmological constant. *Phys. Rev. D* **2013**, *88*, 024016. [[CrossRef](#)]
61. Narzilloev, B.; Rayimbaev, J.; Abdujabbarov, A.; Bambi, C. Charged particle motion around non-singular black holes in conformal gravity in the presence of external magnetic field. *arXiv* **2020**, arXiv:2005.04752.
62. De Laurentis, M.; Younsi, Z.; Porth, O.; Mizuno, Y.; Rezzolla, L. Test-particle dynamics in general spherically symmetric black hole spacetimes. *Phys. Rev. D* **2018**, *97*, 104024. [[CrossRef](#)]
63. Morozova, V.S.; Rezzolla, L.; Ahmedov, B.J. Nonsingular electrodynamics of a rotating black hole moving in an asymptotically uniform magnetic test field. *Phys. Rev. D* **2014**, *89*, 104030. [[CrossRef](#)]
64. Nathanail, A.; Most, E.R.; Rezzolla, L. Gravitational collapse to a Kerr-Newman black hole. *Mon. Not. R. Astron. Soc. Lett.* **2017**, *469*, L31–L35. [[CrossRef](#)]
65. Dadhich, N.; Tursunov, A.; Ahmedov, B.; Stuchlík, Z. The distinguishing signature of magnetic Penrose process. *Mon. Not. R. Astron. Soc* **2018**, *478*, L89–L94. [[CrossRef](#)]
66. Zaslavskii, O.B. Energetics of particle collisions near dirty rotating extremal black holes: Banados-Silk-West effect versus Penrose process. *Phys. Rev. D* **2012**, *86*, 084030. [[CrossRef](#)]
67. Dadhich, N. Magnetic Penrose Process and Blanford-Zanejk mechanism: A clarification. *arXiv* **2012**, arXiv:1210.1041.
68. Abdujabbarov, A.; Ahmedov, B.; Ahmedov, B. Energy extraction and particle acceleration around a rotating black hole in Hořava-Lifshitz gravity. *Phys. Rev. D* **2011**, *84*, 044044. [[CrossRef](#)]
69. Turimov, B.; Toshmatov, B.; Ahmedov, B.; Stuchlík, Z. Quasinormal modes of magnetized black hole. *Phys. Rev. D* **2019**, *100*, 084038. [[CrossRef](#)]
70. Turimov, B.; Ahmedov, B.; Abdujabbarov, A.; Bambi, C. Gravitational lensing by a magnetized compact object in the presence of plasma. *Int. J. Mod. Phys. D* **2019**, *28*, 2040013. [[CrossRef](#)]
71. Ahmedov, B.; Turimov, B.; Stuchlík, Z.; Tursunov, A. Optical properties of magnetized black hole in plasma. *Int. J. Mod. Phys. Conf. Ser.* **2019**, *49*, 1960018. [[CrossRef](#)]

72. de Felice, F.; Sorge, F. Magnetized orbits around a Schwarzschild black hole. *Class. Quantum Gravity* **2003**, *20*, 469–481. [[CrossRef](#)]
73. de Felice, F.; Sorge, F.; Zilio, S. Magnetized orbits around a Kerr black hole. *Class. Quantum Gravity* **2004**, *21*, 961–973. [[CrossRef](#)]
74. Rayimbaev, J.R. Magnetized particle motion around non-Schwarzschild black hole immersed in an external uniform magnetic field. *Astrophys. Space Sci.* **2016**, *361*, 288. [[CrossRef](#)]
75. Rahimov, O.G.; Abdujabbarov, A.A.; Ahmedov, B.J. Magnetized particle capture cross section for braneworld black hole. *Astrophys. Space Sci.* **2011**, *335*, 499–504. [[CrossRef](#)]
76. Rahimov, O.G. Magnetized Particle Motion around Black Hole in Braneworld. *Mod. Phys. Lett. A* **2011**, *26*, 399–408. [[CrossRef](#)]
77. Abdujabbarov, A.; Rayimbaev, J.; Turimov, B.; Atamurotov, F. Dynamics of magnetized particles around 4-D Einstein Gauss-Bonnet black hole. *Phys. Dark Univ.* **2020**, *30*, 100715. [[CrossRef](#)]
78. Rayimbaev, J.; Abdujabbarov, A.; Jamil, M.; Han, W. Dynamics of magnetized particles around Einstein-Æther black hole with uniform magnetic field. *arXiv* **2020**, arXiv:2009.04898.
79. Haydarov, K.; Abdujabbarov, A.; Rayimbaev, J.; Ahmedov, B.. Magnetized Particle Motion around Black Holes in Conformal Gravity: Can Magnetic Interaction Mimic Spin of Black Holes? *Universe* **2020**, *6*, 44. [[CrossRef](#)]
80. Haydarov, K.; Rayimbaev, J.; Abdujabbarov, A.; Palvanov, S.; Begmatova, D. Magnetized particle motion around magnetized Schwarzschild-MOG black hole. *Eur. Phys. J. C* **2020**, *80*, 399. [[CrossRef](#)]
81. Vrba, J.; Abdujabbarov, A.; Kološ, M.; Ahmedov, B.; Stuchlík, Z.; Rayimbaev, J. Charged and magnetized particles motion in the field of generic singular black holes governed by general relativity coupled to nonlinear electrodynamics. *Phys. Rev. D* **2020**, *101*, 124039. [[CrossRef](#)]
82. Zipoy, D.M. Topology of Some Spheroidal Metrics. *J. Math. Phys.* **1966**, *7*, 1137–1143. [[CrossRef](#)]
83. Voorhees, B.H. Static Axially Symmetric Gravitational Fields. *Phys. Rev. D* **1970**, *2*, 2119–2122. [[CrossRef](#)]
84. Turimov, B.; Ahmedov, B.; Kološ, M.; Stuchlík, Z. Axially symmetric and static solutions of Einstein equations with self-gravitating scalar field. *Phys. Rev. D* **2018**, *98*, 084039. [[CrossRef](#)]
85. Bambi, C. Testing black hole candidates with electromagnetic radiation. *Rev. Mod. Phys.* **2017**, *89*, 025001. [[CrossRef](#)]
86. Mazur, P.O.; Mottola, E. Gravitational vacuum condensate stars. *Proc. Natl. Acad. Sci. USA* **2004**, *101*, 9545–9550. [[CrossRef](#)]
87. Chirenti, C.B.M.H.; Rezzolla, L. How to tell a gravastar from a black hole. *Class. Quantum Gravity* **2007**, *24*, 4191–4206. [[CrossRef](#)]
88. Chirenti, C.; Rezzolla, L. Did GW150914 produce a rotating gravastar? *Phys. Rev. D* **2016**, *94*, 084016. [[CrossRef](#)]
89. Cardoso, V.; Franzin, E.; Pani, P. Is the Gravitational-Wave Ringdown a Probe of the Event Horizon? *Phys. Rev. Lett.* **2016**, *116*, 171101; Erratum in **2016**, *117*, 089902. [[CrossRef](#)]
90. Carballo-Rubio, R.; Di Filippo, F.; Liberati, S.; Visser, M. Phenomenological aspects of black holes beyond general relativity. *Phys. Rev. D* **2018**, *98*, 124009. [[CrossRef](#)]
91. Rayimbaev, J.; Figueroa, M.; Stuchlík, Z.; Juraev, B. Test particle orbits around regular black holes in general relativity combined with nonlinear electrodynamics. *Phys. Rev. D* **2020**, *101*, 104045. [[CrossRef](#)]
92. Vrba, J.; Abdujabbarov, A.; Tursunov, A.; Ahmedov, B.; Stuchlík, Z. Particle motion around generic black holes coupled to non-linear electrodynamics. *Eur. Phys. J. C* **2019**, *79*, 778. [[CrossRef](#)]
93. Stuchlík, Z.; Kološ, M.; Kovář, J.; Slaný, P.; Tursunov, A. Influence of Cosmic Repulsion and Magnetic Fields on Accretion Disks Rotating around Kerr Black Holes. *Universe* **2020**, *6*, 26. [[CrossRef](#)]
94. Benavides-Gallego, C.A.; Abdujabbarov, A.A.; Bambi, C. Gravitational lensing for a boosted Kerr black hole in the presence of plasma. *Eur. Phys. J. C* **2018**, *78*, 694. [[CrossRef](#)]
95. Mori, K.; Gotthelf, E.V.; Zhang, S.; An, H.; Baganoff, F.K.; Barrière, N.M.; Beloborodov, A.M.; Boggs, S.E.; Christensen, F.E.; Craig, W.W.; et al. NuSTAR Discovery of a 3.76 s Transient Magnetar Near Sagittarius A*. *Astron. J. Lett.* **2013**, *770*, L23. [[CrossRef](#)]
96. Chandrasekhar, S. *The Mathematical Theory of Black Holes*; Oxford University Press: New York, NY, USA, 1998.

97. Grib, A.A.; Pavlov, Y.V. On particle collisions near rotating black holes. *Gravit. Cosmol.* **2011**, *17*, 42–46. [[CrossRef](#)]
98. Grib, A.A.; Pavlov, Y.V. On particle collisions in the gravitational field of the Kerr black hole. *Astropart. Phys.* **2011**, *34*, 581–586. [[CrossRef](#)]

Publisher’s Note: MDPI stays neutral with regard to jurisdictional claims in published maps and institutional affiliations.



© 2020 by the authors. Licensee MDPI, Basel, Switzerland. This article is an open access article distributed under the terms and conditions of the Creative Commons Attribution (CC BY) license (<http://creativecommons.org/licenses/by/4.0/>).